

PACS numbers: 42.82.Et, 41.75.Ht, 42.62. – b

EFFECT OF THE FOCUSING MAGNETOSTATIC FIELD PROFILE ON THE DIFFRACTION RADIATION OSCILLATOR EXCITATION

A.I. Tsvyk, E.V. Belousov, V.N. Zheltov, A.V. Nesterenko, E.M. Khutoryan

Usikov Institute of Radiophysics and Electronics of NAS of Ukraine,
12, Ak. Proskury Str., 61085, Kharkiv, Ukraine
E-mail: gdr@ire.kharkov.ua

Effect of the focusing magnetostatic field (FMF) profile on the output characteristics of diffraction radiation oscillator (DRO) is studied experimentally. The laboratory prototype of the mm range DRO produced in IRE NAS of Ukraine was used in the research. Peculiarities of the output power, oscillation frequency, starting current and other DRO characteristics for the cases of the decreasing, sagging and increasing magnetostatic field along the direction of the electron flow motion were determined. Prospects for the use of the increasing FMF in DRO are shown.

Keywords: SOURCE OF ELECTROMAGNETIC OSCILLATIONS, MILLIMETER WAVES, SMITH-PURCELL RADIATION, DIFFRACTION RADIATION OSCILLATOR (DRO), OPEN RESONATOR.

(Received 20 November 2009, in final form 05 December 2009)

1. INTRODUCTION

The actual problem of microwave electronics is the creation of nonrelativistic high-stable sources of electromagnetic oscillations in the frequency range higher than 300 GHz (short-wave range). Diffraction radiation oscillators (DRO), where the Smith-Purcell radiation of an electron flow (EF) in an open resonator (OR) with diffraction grating [1-3] is used, are developing in this direction. Up to now, the experimental investigation of DRO was mainly performed in the mm range (on the frequencies < 300 GHz) with uniform focusing magnetostatic field (FMF) [1, 2]. Experimentally established, the DRO starting current increases with the shortening of the wavelength that is connected with the increase in the ohmic losses in electrodynamic system of oscillator and with the decrease in the EF effective thickness $2z_{\min} = \lambda\beta/\pi$ ($2z_{\min} < 0,03$ mm for the frequencies > 300 GHz). Actually in the short-wave range the EF thickness in DRO $2z_q$ may exceed several times the value of $2z_{\min}$ ($2z_q > 2z_{\min}$, “thick” EF), at the same time the change in shape and EF structure in the interaction space [4] can substantially influence the oscillator excitation. Therefore, to create DRO in the short-wave range the further development of the theory and experimental investigation of such oscillators is required.

Assumed, the DRO output characteristics with “thick” ribbon EF can be substantially improved if use the non-uniform FMF [2, 3] for the electron beam focusing. In particular, in accordance with the aforesaid in IRE NAS of Ukraine the laboratory prototype of DRO-LMH with the local magnetostatic heterogeneity of the focusing field in the interaction space [5] was

proposed, studied and created. Shown, in DRO-LMH with the flow thickness of $2z_q \approx 1,7 (2z_{\min})$ and the current density of 10 A/cm^2 in the frequency range of 56-80 GHz the generation power increases about two times, the starting current of oscillator decreases, and the long-term frequency stability is improved by one order in contrast to the case of the uniform FMF. However, the possibilities of improvement of the DRO output characteristics by the FMF profiling in the interaction space are poorly studied up to now.

In the paper we present the results of the experimental investigation of DRO with different FMF profiles on the EF axis; the decreasing, sagging (symmetric) and increasing FMF along the direction of the electron flow motion. Prospects for the development of DRO with the increasing FMF profile are shown.

2. STATEMENT OF THE PROBLEM

The laboratory prototype of DRO produced in IRE NAS of Ukraine by B.K. Skrynnik [1] is studied experimentally. This DRO contains the diode electron gun of ribbon EF (cross-section is $5 \times 0,2 \text{ mm}^2$, flow thickness is $2z_q = 0,2 \text{ mm}$, $2z_{\min} \approx 0,14 \text{ mm}$, the current density is $5\text{-}10 \text{ A/cm}^2$); spherocylindrical OR with diffraction grating; oscillator operates in the frequency range $f = 58\text{-}70 \text{ GHz}$ at voltages $U_a = 1600\text{-}2500 \text{ V}$. Device is placed between the round (conic) pole tips (N_1, N_2) of electromagnet, where non-uniform magnetostatic field is generated for the flow focusing (Fig. 1a, b).

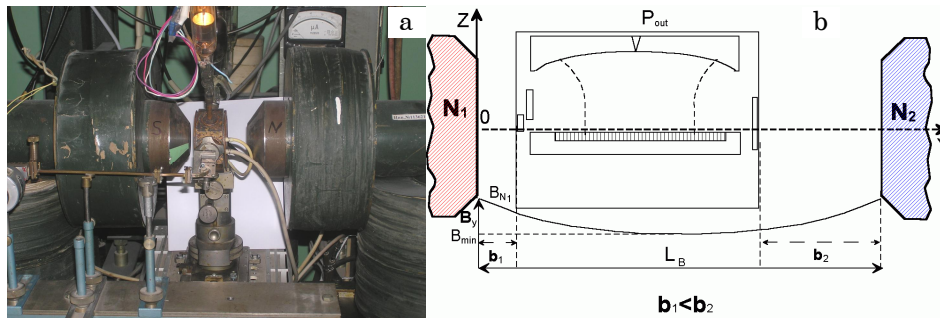


Fig. 1 – Experimental setup (a) and the scheme of DRO arrangement in non-uniform magnetic field between the pole tips of electromagnet (b)

Origin of the rectangular coordinate system XYZ is chosen in the center of the pole tip N_1 ; the OY -axis is directed along the N_1N_2 -axis of the pole tips (EF); the OX -axis – along the EF width (parallel to the grating grooves); the OZ -axis – along the EF thickness (perpendicular to the grating surface and parallel to the OR axis). Here we denote: D_N is the diameter of magnet tips; L_B is the distance between the tips; $\Delta = 40 \text{ mm}$ is the thickness of the device body along the OY -axis; b_1 is the distance between the tip N_1 and the left face of the device body (nearby this face inside the device there is the cathode of the electron gun; $y_k \approx b_1$); b_2 is the distance between the tip N_2 and the right face of the device (electron collector, $y_{kol} = L_b - b_2$). Displacing the device with respect to the symmetry plane $y = L_b/2$ of the magnet to the left ($b_1 < b_2$, $z = 0$, Fig. 1b), to the right ($b_1 > b_2$, $z = 0$), downward ($z < 0$) or arranging it symmetrically with respect to the pole tips ($b_1 = b_2$, $z = 0$),

we can create different profiles of magnetostatic field for the EF focusing. The value of the magnetic induction $|\vec{B}|$ between the pole tips is driven by the electromagnet-coil current. Electromagnet with the device has special adjusting mechanism, which allows with high accuracy (up to $\pm 0,08$ min) to determine the inclination angle $\psi = \pm \arctg[2z_{sh}/(L_B + A)]$ (in minutes, where $A = \text{const} = 758$ mm) of the longitudinal axis N_1N_2 of the pole tips to the axial plane $z = 0$ (of ribbon EF); z_{sh} is the displacement of the tips N_1, N_2 with respect to the plane $z = 0$ (at ψ degrees rotation) and is determined by the micrometer.

3. ANALYSIS OF THE DRO FOCUSING MAGNETOSTATIC FIELD

In Fig. 2 we present the experimental (crosses) dependence of the longitudinal field component $B_y(0, y, 0)$ along the N_1N_2 -axis of electromagnet tips (Fig. 1a), where the DRO investigation was carried out ($L_B = 82$ mm, $D_N = 50$, $\psi = 0$); this dependence is approximated by the theoretical (solid line) curve [4]

$$B_y(y) = B_N * f(y); f(y) = 1 - \xi \sin(\pi y/L_B), \quad (1)$$

where B_N is the magnetic induction on the pole tips ($y = 0$; L_B); $\xi = (B_N - B_{min})/B_N$ is the parameter of the FMF non-uniformity.

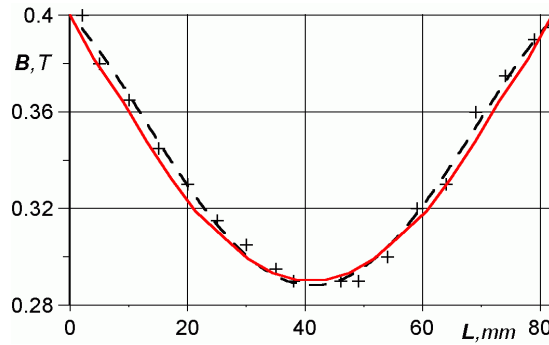


Fig. 2 – “Sagging” of the component $B_y(0, y, 0)$ of magnetostatic field along the N_1N_2 -axis of electromagnet tips (Fig. 1a): experiment (crosses), theory (solid line)

It is seen that the field component B_y on the axis between the pole tips “sags” with the minimum $B_{min} = 0,29$ T in the plane $y = L_B/2$ with the value $\xi \approx 0,275$. Experimental measurements show that the “sagging” depth $B_y(y)$ increases with the decrease in the tip diameter D_N and the increase in the distance L_B between the tips.

Knowing the axial component B_y of the field $\vec{B}(b_x, b_y, b_z)$, from the solution of the Laplace equation for magnetostatic potential φ_B and the relation $\vec{B} = -\text{grad}\varphi_B$, it is easy to determine the field components b_x, b_y, b_z and the lines of force in any point (x, y, z) of the space between the pole tips [4].

In particular, in the paraxial approximation (nearby the OY -axis) the force line projection $z_B(y, z_N)$ of the vector $\vec{B}(b_x, b_y, b_z)$ on the plane ZOY and the values of b_z and $|\vec{B}_{yz}|$ on this line are determined from the relation

$$z_B(y, z_N) = \frac{z_N}{\sqrt{f(y)}}; \quad b_z(y, z_N) = -\frac{1}{2} B_N z_N \frac{f'(y)}{\sqrt{f(y)}}; \quad |\bar{B}_{zy}| = \sqrt{b_z^2(y, z_N) + B_y^2(y)}, \quad (2)$$

where z_N is the initial coordinate of $z_B(0, z_N)$ on the pole tip N_1 of magnet; stroke denotes the derivative of the y -component.

As seen from (2), in the region $z > 0$ the curve $z_B(y)$ is "convex", and in the region $z < 0$ it is "sagging" relative to the axial plane $z = 0$. In the plane $y = L_B/2$ on the curve $z_B(y)$ the values are $B_y = B_{\min}$ and $b_z = 0$, and during the transmission through this plane the magnetic field reversion (sign reversal of the component $b_z(y)$) is observed. On the N_1N_2 -axis $z_N = 0$, i.e., the line of force is directed along the OY -axis with the field vector $\bar{B}(0, B_y, 0)$.

The mean field (1) between the cathode ($y = y_k$) and the collector ($y = y_{kol}$) in the device is found as

$$\bar{B}_y = B_N \bar{f}_y; \quad \bar{f}_y = 1 - \xi \frac{2L_B}{\pi d_{kL}} \cos \frac{\pi(b_1 + b_2)}{2L_B} \cos \frac{\pi(b_1 - b_2)}{2L_B}, \quad y_k < y < y_{kol}, \quad (3)$$

where $d_{kL} = d_k + d_a + 2a$; d_{kL} is the distance between the cathode and the electron collector; d_k is the distance between the cathode and the anode slot; d_a is the length of the anode slot (thickness of the anode lath); $2a$ is the length of the OR mirror with the grating along the OY -axis. If $b_1 = b_2$ then (3) defines the mean value of the "sagging" field (1), which is symmetric with respect to the plane $y = L_B/2$ in the range of $[y_k, y_{kol}]$ of EF movement; if $b_2 = L_B/2$ then it defines the mean value of the decreasing field B_y in the range of $[y_k \approx b_1, y_{kol} = L_B/2]$, and at $b_1 = L_B/2$ - of the increasing field B_y in the range of $[y_k = L_B/2, y_{kol} = L_b - b_2]$. If b_1 and $b_2 \neq L_B/2$ then in the range of $[y_k, y_{kol}]$ the field B_y decreases (or increases) with the field minimum B_{\min} in the plane $y = L_B/2$.

Solving the equation of electron motion by the partial region method with the averaged field \bar{B}_y , in the first approximation it is possible to estimate the level of influence of the parameter ξ on the electron motion trajectories and the EF structure [4]. In such a way one can obtain the more exact analytical formulas for the electron motion trajectories in non-uniform FMF, if present the field (1) as the staircase function in the equation of electron motion

$$B_y(y) = B_N \sum_{n=0}^N \bar{f}_n(y) G(y), \quad (4)$$

where $\delta = L_B/N \ll \bar{\lambda}_c$ is the length of the field stair; N is the number of stairs; $\bar{f}_n = (1/\delta) \int_{y_n}^{y_{n+1}} f(y) dy$ is the mean of function $f(y)$ on the n -th stair; $G(y)$ is the unit function, which is equal to 1 in the range of $[y_n, y_{n+1}]$ and 0 outside of this range; $\bar{\lambda}_c$ is the cyclotron electron wavelength in the averaged field \bar{B}_y .

In Fig. 3 we present curves, which show the general view of the boundary electron motion trajectories in the ZOY-plane nearby the grating surface with non-uniform field (4). Trajectories were calculated at the following values: $\xi = 0,1; 0,3$ for EF with the parameters: $S_k = 5 \times 0,2 \text{ mm}^2$ is the flow cross-section on the cathode; $2z_q = 0,2 \text{ mm}$ is the flow thickness; $B_N = 0,4 \text{ T}$; $U_a = 2500 \text{ V}$; $j = 10 \text{ A/cm}^2$ is the current density from the cathode (analytical theory and study of the EF formation in the interaction space between DRO and non-uniform field (4) will be considered in another work).

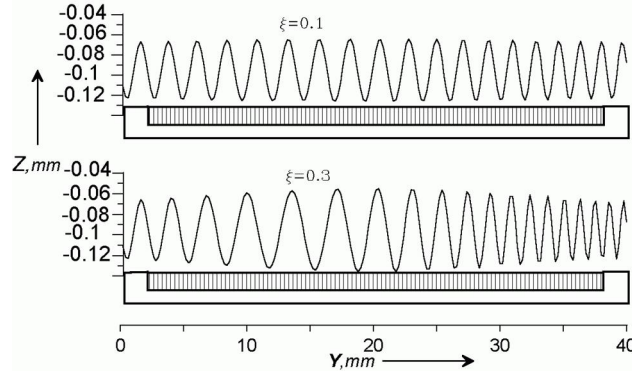


Fig. 3 – Projection of the electron motion trajectory in the ZOY-plane nearby the surface of OR mirror with the grating in non-uniform field (4) with non-uniformity parameters $\xi = 0,1; 0,3$

As seen from Fig. 3, during the electron motion in the decreasing field B_y ($b_1 < y < L_b/2$) the wavelength and the pulsation amplitude of electron trajectory increase, and in the increasing field ($L_b/2 < y < b_2$) they decrease; as a result in the decreasing field electrons approach to the grating surface, and in the increasing one they move away from the grating. Obviously, these changes in the electron motion trajectories can lead to the increase or decrease in the interaction efficiency between the EF and the resonator field of DRO. This is confirmed by the performed experimental investigations.

4. EXPERIMENTAL INVESTIGATIONS

We experimentally investigate DRO in the cases when it is placed in the decreasing field B_y ($0 < y < L_B/2$); in the sagging field ($b_1 = b_2$; $-b_1 + L_B/2 < y < (L_B - b_1)$) and in the increasing one ($L_B/2 < y < L_B$). Depending on the device arrangement in the field B_y , we conditionally denote the following:

- DRO(A) – device with the sagging (symmetric) FMF profile; according to the curve in Fig. 2 in this oscillator the EF focusing is realized by the relatively low magnetostatic field B_y , which in the area of the anode-collector has the boundary parameters $B_y(y_a) = B_y(y_{kol}) = 0,32 \text{ T}$; $B_{\min} = 0,29 \text{ T}$; $\xi_A = 0,094$; $b_1 = b_2 = 20 \text{ mm}$;
- DRO(B) – with the decreasing profile of the field B_y with the boundary parameters $B_y(y_a) = 0,4 \text{ T}$; $B_y(y_{kol}) = 0,29 \text{ T}$; $\xi_B = 0,275$; $b_1 = 0$; $b_2 = 40 \text{ mm}$;
- DRO(C) – with the increasing profile of the field B_y with the boundary parameters $B_y(y_a) = 0,29 \text{ T}$; $B_y(y_{kol}) = 0,4 \text{ T}$; $\xi_B = 0,275$; $b_1 = 40$; $b_2 = 0 \text{ mm}$.

We experimentally study the output characteristics of DRO(A, B, C), namely, the generation power ($P_0 = P/P_{\max}$), electron frequency tuning within the generation zone, starting current ($I_s = I/I_{s,\min}$) and other characteristics at different values of ψ , B_N , U_a . Some investigation results are presented in Fig. 4-7 in the case of the single-mode oscillation excited in the DRO resonator.

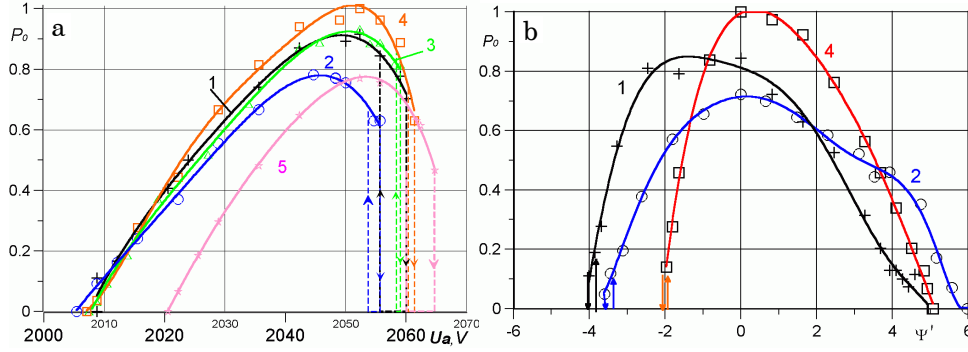


Fig. 4 – Effect of the FMF profile on the DRO excitation within the generation zones with respect to the voltage U_a (a) and the angle ψ (b)

In Fig. 4 for DRO(A, B, C) we show the dependences of the power P_0 on the accelerating voltage U_a within the generation zone: DRO(A) – the curve 1 at the values $b_1 = b_2 = 20$ mm; DRO(B) – the curves 2 and 3 correspond to the values $b_1 = 10$ mm; $b_2 = 30$ mm and $b_1 = 0$ mm, $b_2 = 40$ mm; DRO(C) – the curves 4 and 5 correspond to the values $b_1 = 30$ mm, $b_2 = 10$ mm and $b_1 = 40$ mm, $b_2 = 0$ mm; here $B_N = 0,4$ T; $f_0 = 52,083$ GHz and $\lambda = 5,76$ mm are the oscillation frequency and the wavelength at $U_a = 2050$ V, respectively; if U_a changes in the generation zone, the adjustment of the angle ψ on the maximum power P_0 is executed; $P_{\max} = 500$ mW.

As follows from the analysis of Fig. 4a and other experimentally obtained results:

- in DRO(A, B, C) the physical principles of oscillation excitation within the generation zone with respect to the voltage keep: the soft oscillation mode in the beginning of this zone and the hard mode of oscillation suppression ($U_a = U_1$); the oscillation excitation in the end of the generation zone ($U_a = U_1 - \delta U_a$), where δU_a is the hysteresis loop width [6];
- in DRO(A) the change in the output power (curve 1, Fig. 4a) versus the voltage U_a in the generation zone is almost the same as in DRO with uniform B_0 [1]. However, DRO(A) operates at lower FMF with the starting value $B_{start} = 0,29$ T, while in uniform field $B_{start} = 0,38-0,4$ T;
- in DRO(B) with the increase of the field downhill slope in the direction of EF motion the power and the width of the generation zone increase, the hysteresis loop width δU_a decreases, and here the maximum value of P_0 in the generation zone (curve 3) does not exceed the maximum power of DRO(A) (curve 1). Comparison of the curves 1 and 3 gives that the hysteresis loop width δU_a of DRO(A) (curve 1) substantially exceeds the value of δU_a of the curve 3, i.e., DRO(B) within the hard mode of oscillation suppression ($U_a = U_1$) is started at the negligible decrease in the voltage U_1 ;

- in DRO(C) the increase in the generation power (curve 4) as compared with DRO(A, B) (curves 1 and 3) is observed; and here, as in DRO(B), the hysteresis loop width δU_a decreases in the generation zone. So, in DRO it is promising to use the increasing FMF in the direction of EF motion to increase the generation power.

Dependences in Fig. 4b represent the peculiarities of the output power (P_0) change in DRO(A, B, C) versus the angle ψ at the parameters $U_a = 2050$ V; $B_N = 0,4$ T; $\lambda = 5,76$ mm. Analysis of these curves show:

- electromagnetic oscillations in DRO(A, B, C) are excited in a certain range $\Delta\psi$ of the angle ψ change; the value of $\Delta\psi = \psi_2 - \psi_1$ defines the width of the generation zone with respect to the angle ψ , where ψ_1 and ψ_2 are the boundary values of the angles of the beginning and suppression of oscillations in the generation zone;
- change in the FMF profile leads to the displacement of the optimal value of the angle $\Delta\psi = \psi_{opt}$ for the maximum generation power and to the change in the width $\Delta\psi$ of the generation zone;
- DRO(C) (the increasing FMF) has more narrow zone $\Delta\psi$ and the increased generation power (curve 4, Fig. 4b) than in DRO(A, B) (curves 1 and 2 in Fig. 4b);
- in DRO(A, B, C) the hysteresis with respect to the angle ψ , where $\delta\psi$ is the hysteresis loop width, is found in the beginning of the generation zone ($\psi = \psi_1 - \delta\psi$).

In Fig. 5 for DRO(A) with the parameter $\xi = 0,01$ (quasi-homogeneous field, $B_{min} = B_N$) we present the dependences of the output power P_0 and the shift $F = f - f_0$ of the oscillation frequency f on the FMF (B_N) at different angles ψ ; here $f_0 = 52,083$ GHz; curves 1, 2, 3, 4 correspond to the values $\psi = 7,849, 8,531, 9,943, 11,355$, respectively. As seen, the device operates at the magnetic field $B > B_{start} = 0,42$ T; at first, for the given ψ with the increase in B up to the value B_{opt} the increase in the output power up to the maximum value P_{max} and the decrease of the oscillation frequency shift F are observed, and then at $B > B_{opt}$ – the decrease in P_0 and slight change in F . Maximum power in oscillator is achieved at the value $\psi = 9,943$ (curve 3), which approximately corresponds to the angle ψ_{opt} in Fig. 4. Note, in the theory of DRO [1] the output power P_0 is proportional to $P_a(\varphi_c)$, and the frequency shift F is determined by the relation $F = f_0 P_r(\varphi_c) / (2Q P_a(\varphi_c))$, where Q is the OR quality-factor; $P_a(\varphi_c)$ and $P_r(\varphi_c)$ are, respectively, the active and the reactive components of the interaction power between the EF and the OR electromagnetic field nearby the grating surface; φ_c is the cyclotron angle of electron transit into the resonator field. Therefore, observed in Fig. 4,5 changes in P_0 and F are explained by the variation of the interaction power between the EF and the OR electromagnetic field under the increase of magnetostatic field. Practically, with the change in B_N (or U_a) the adjustment of the angle ψ on the maximum generation power is executed; as a result we obtain the smooth curves of the dependences of P_0 and F on B_N with the “saturation” $P_0 = P_{max}$ in the “roll-off” region of the curves 1-3 in Fig. 5 at $B > B_{opt}$ (for the first time the possibilities of “alignment” of the dependence of P on magnetic field B by the inclination angle ψ in DRO are shown in [7]).

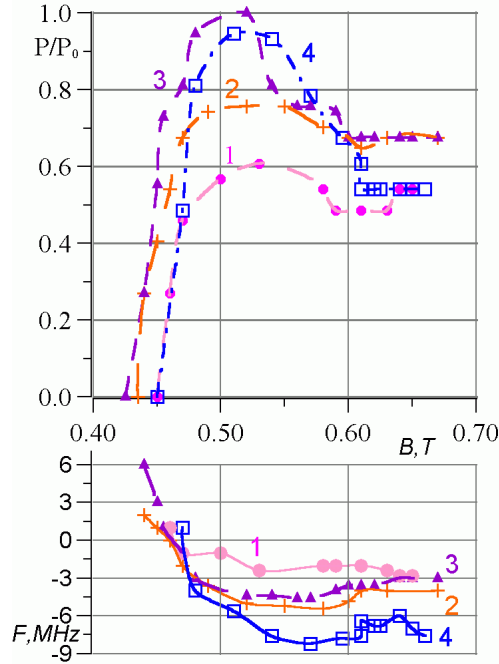


Fig. 5 – Dependences of the output power and the frequency in DRO(A) on the magnetic field B_N at different angles ψ ; curves 1, 2, 3, 4 correspond to $\psi = 7, 849, 8, 531, 9, 943, 11, 355$, respectively

In Fig. 6 for DRO(A) we present the dependences of the starting current $i_s = I_s/I_{s,min}$ (curve 1), power P_0 (curve 2), coefficient $K_i = I_{kol}/I_k$ of the EF transmission to the collector (curve 3) on the normalized angle ψ/ψ_{opt} ; curve 4 is the theoretical one for i_s in the averaged field (3) calculated with analytical formulas [8]; here we denoted: $I_{s,min}$ is the minimum of the starting current; I_{kol} is the collector current; I_k is the cathode current. If $\psi = 0$ then EF moves parallel to the grating plane without electron precipitation on its surface; at $\psi = \psi_1$ – the “weak” electron precipitation in the beginning of the generation zone; at $\psi = \psi_2$ – the “strong” EF precipitation in the end of the generation zone. Comparison of the curves 1 and 4 gives satisfactory fit of the theory and experiment for the starting current, and in this case the optimal value of the angle ψ_{opt} for the power P_{0max} does not coincide with the optimal angle ψ_{oi} for $I_{s,min}$ (in the given case $\psi_{opt} = 1,1\psi_{oi}$). Besides, in the generation zones with respect to the angle ψ (Fig. 4b and Fig. 6) the evident asymmetry of the curves P_0 and i_s relative to the angle ψ_{opt} is observed; and in the generation zone of DRO(A) (curve 1, Fig. 4b) the value ψ_{opt} is shifted to the left (to the beginning of the generation zone, $\psi = \psi_1$), and on the curves 1, 2 and 4 (Fig. 6) it is shifted to the right, to the end of the generation zone ($\psi = \psi_2$).

Analysis shows that the change in symmetry and shape of the generation zones with respect to the angle ψ in DRO(A, B, C) is mainly determined by the conditions of EF input into the interaction space of oscillator (“spot” 2r on the grating surface of electromagnetic oscillation excited in OR; r is the

spot radius, [1]). In particular, in Fig. 7 we present the photo of the trail of the electron precipitation on the grating surface of DRO(A) in the case of $\psi = \psi_{opt}$, which is obtained in the laboratory prototype of oscillator with the demountable design (here the field value B_{min} is nearby the axial plane $y = y_{or} = L_B/2$ of oscillator). Established that DRO(A) has maximum power when electrons precipitate mainly on the surface of the OR mirror with the grating on the anode side of the electron gun ($y_a < y < y_{or}$) and slightly – on the second part of the grating surface on the collector side ($y_{or} < y < y_{kol}$).

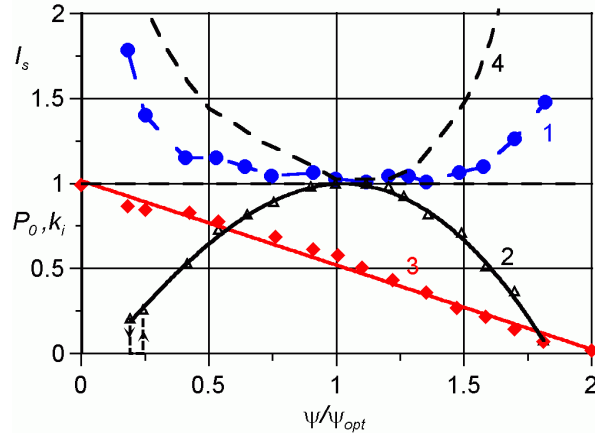


Fig. 6 – Effect of the angle ψ_{opt} in DRO with the sagging (symmetric) profile of FMF on the starting current I_s (curve 1), the output power P_0 (curve 2) and the coefficient K_i of the EF transmission to the collector (curve 3); curve 4 is the theoretical one for the starting current

In DRO(B) the optimal conditions of the EF precipitation on the grating surface substantially depend on the downhill slope of the field B_y and the value of the non-uniformity parameter ξ (in such oscillator the field value B_{min} is shifted relative to the plane $y = y_{or}$ towards the electron collector). In particular, at “large” values of ξ ($\xi = 0,2-0,3$, Fig. 2, 3) electrons precipitate on the grating in the range $y_{or} < y < y_{kol}$, and as a result the “dark” and the “light” luminescence regions of the trail of electron precipitation in Fig. 7 will change places; at small values of the parameter ξ ($\xi = 0,1-0,15$) electrons precipitate along the whole grating length (the “clinotron” conditions [8, 9]).

Anode ($y = y_a$)

Collector ($y = y_{kol}$)



Fig. 7 – Photo of the trail of the electron precipitation on OR mirror with the grating in DRO(A) in the case of the maximum output power ($\psi = \psi_{opt}$; curve 2, Fig. 6)

In DRO(C) the field value B_{\min} is shifted towards the plane $y = y_a$ of the electron gun anode. Therefore here in the optimal conditions ($\psi = \psi_{opt}$) electrons precipitate mainly on the surface of OR mirror on the anode side, but in the smaller region ($y_a < y < y_{or} - r$) than in Fig. 7, and slightly – in the interaction space $2r$, since in the direction of EF motion the pulsation amplitude of the motion trajectory of boundary electrons decreases (Fig. 3). It is important to note that in the case of the “thick” EF the electron layer of the thickness of $2z_{\min}$ is the most effective one in DRO(C), that decreases the conversion efficiency of the device. However, the efficiency of use of the “thick” EF in this device can be substantially increased, if introduce the local magnetostatic heterogeneity of the field [5] into the interaction space. Discovered in DRO(C) phenomena of the generation power increase (Fig. 4) in the conditions of the “weak” electron precipitation in the interaction space (surface of the microperiodic grating) indicate the prospects for the development of this oscillator in the frequency range higher than 300 GHz.

5. CONCLUSIONS

The output characteristics of three DRO modifications, which differ by the FMF profile: DRO(A) – with the sagging (symmetric) field, DRO(B) – with the decreasing field, DRO(C) – with the increasing magnetostatic field in the direction of EF motion are experimentally studied. The new phenomena are discovered and the specific peculiarities of the DRO output characteristic change on the FMF profile are established:

- With the change of the FMF profile the typical for DRO conditions of oscillation excitation within the generation zone with respect to the voltage keep: (1) – the soft oscillation mode in the beginning of this zone and the hard mode of oscillation suppression; (2) – the oscillation excitation in the end of the generation zone.
- The FMF profile change in DRO can lead to the substantial decrease in the hysteresis loop width in the generation zone with respect to the voltage in the region of the hard oscillation mode.
- Electromagnetic oscillations in DRO(A, B, C) are excited in a certain range $\Delta\psi$ of the inclination angle ψ change (the axial force line angle of FMF to the axial plane of ribbon flow); in the generation zone with respect to the angle ψ the hysteresis effect is discovered, which is observed in the beginning of the generation zone in conditions of the minimum electron precipitation on the grating surface.
- In DRO with the sagging FMF profile the starting value of magnetostatic field decreases in comparison with the uniform field.
- Effect of the generation power increase in DRO with the increasing FMF profile at the minimum EF precipitation on the grating surface (the interaction space) is discovered.
- Investigation results imply about the prospects for the development of DRO with non-uniform FMF in the frequency range higher than 300 GHz.

REFERENCES

1. *Generatory difraktsionnogo izlucheniya* (Red. V.P. Shestopalov) (K.: Nauk. dumka: 1991).
2. A.I. Tsvyk, *Razvitie difraktsionnoy elektroniki (dostizheniya i problemy). Radiofizika i elektronika*, 550 (Kharkov: IRE NAN Ukrainy: 2005).

3. A.A. Shmatko, *Elektronno-volnovye sistemy millimetrovogo diapazona. Tom 1* (Kharkov: KhNU im. V.N. Karazina: 2008)
4. A.I. Tsvyk, E.V. Belousov, A.V. Nesterenko, V.N. Zheltov, *Visnyk SumDU. Seriya Fizyka, matamatyka, mehanika*, No2, 167 (2008).
5. A.I. Tsvyk, G.S. Borobjov, A.V. Nesterenko, V.N. Zheltov, *Radiofizika* **43** No2, 144 (2000).
6. G.S. Borobjov, A.I. Tsvyk, *Radiofizika* **25** No9, 1060 (1982).
7. V.V. Nerubenko, A.I. Tsvyk, *Radiotekhnika* **19**, 107 (1971).
8. A.I. Tsvyk, *Radiofizika* **21** No8, 1216 (1978).
9. *Klinotron* (Red. A.Ya. Usikov) (K.: Nauk. dumka: 1992).